Negative acoustic radiation force induced on an elastic sphere by laser irradiation

Hai-Qun Yu,[1] Jie Yao,[1] Da-Jian Wu,[1,*] Xue-Wei Wu,[2] and Xiao-Jun Liu[2,†]

[1]*Jiangsu Key Lab on Opto-Electronic Technology, School of Physics and Technology, Nanjing Normal University, Nanjing 210023, China*

[2]*Key Laboratory of Modern Acoustics, School of Physics, Nanjing University, Nanjing 210093, China*

(Received 23 July 2018; revised manuscript received 31 October 2018; published 26 November 2018)

We propose an alternative strategy to modulate the acoustic radiation force (ARF) acting on an elastic sphere (ES) using laser irradiation. A mathematical model of the interaction of the acoustic plane wave with the laser-irradiated ES is developed to calculate the ARF acting on the ES. It is demonstrated that the action of this laser-induced photoacoustic effect on a polystyrene (PS) sphere could strongly affect the ARFs of acoustic plane waves that are incident on the PS sphere and negative ARFs could thus be realized. The variational ARF behavior observed is ascribed to competition between the photoacoustic effect and the acoustic scattering. Furthermore, we find that both the laser intensity and the phase difference between the incident laser beam and the acoustic plane wave could be used to modulate the ARF acting on the irradiated PS sphere, with the phase difference playing the dominant role. One effective method for control of the negative ARF involves changing the laser intensity with a suitable phase difference. The work presented here may lead to an alternative way to perform single-beam acoustic manipulation.

DOI: 10.1103/PhysRevE.98.053105

I. INTRODUCTION

Acoustic manipulation offers advantages that include contactless and nondestructive operation, and its versatility has seen this technique find wide application in fields such as drug delivery [1], cell screening and separation [2], microassembly systems [3,4], and gene therapy [5]. The core aspect of acoustic manipulation is the acoustic radiation force (ARF) [6,7]. In general, the ARF of a plane acoustic wave that acts on a particle is a pushing force. To improve both the flexibility and the feasibility of acoustic manipulation techniques, several different methods have been explored in attempts to generate attractive ARFs. For example, Mitri [8] reported that a high-order Bessel beam can generate an attractive ARF on a fluid or a solid sphere. In the field of spherically diverging sound, the ARF that acts on a rigid sphere becomes an attractive force when the sphere is located relatively close to the source [9]. For focused Gaussian acoustic beams, when a particle deviates from the axial focal point, an attractive ARF can also be obtained because of the competition between the scattering force and the gradient force [10–13]. Shen and Wang [14] developed a model for the ARF that is exerted by standing surface acoustic waves acting on a rigid cylinder. Their model shows that standing surface acoustic waves can also generate an attractive ARF and that the magnitude and direction of this ARF are influenced by the Rayleigh angle. In addition, Mitri and Fellah [15] found that, for an elastic sphere that has been coated with a polymer-type viscoelastic shell, the sound absorption properties of the polymer layer can induce an attractive ARF. Baresch *et al.* [16] reported the experimental realization of a pulling effect on elastic particles in water produced by a focused acoustic vortex beam experimentally. In contrast, a regular airborne acoustic vortex was found to be suitable only for trapping Rayleigh particles [17], while Marzo *et al.* [18] used rapidly time-multiplexed acoustic vortices to achieve stable trapping of Mie particles. Recently, Rajabi and Mojahed [19,20] proposed use of a three-layered sphere with an active inner piezoelectric layer to realize an attractive ARF. By varying the voltage across the inner piezoelectric layer, this active three-layered shell can vibrate in specific modes and the surrounding acoustic fields can thus be changed [21–23]. The ARF acting on the active shell could then be transformed from a repulsive state to an attractive state. However, the operation required on the inner piezoelectric layer is difficult to perform, which hampers further applications of the sphere.

The photoacoustic effect, which is the formation of acoustic waves as a result of light absorption in an object, has been used extensively in applications including tissue imaging [24], nondestructive defectoscopy [25], and high-frequency ultrasound generation [26]. The most common and dominant mechanism for the photoacoustic effect is the thermoelastic regime [27]. When an object is irradiated using a laser beam, the absorbed laser energy is converted into heat and this causes an immediate temperature rise in the object. The elastic vibrations generated in this object as a result of thermal expansion then emit acoustic waves. It was found that the object's vibration behavior could be controlled effectively by varying the laser parameters [28,29], which may offer an alternative way to control the ARF that acts on an object.

In this paper, we propose a strategy to modulate the ARF acting on an elastic sphere (ES) using laser irradiation. A mathematical model of a plane acoustic wave interacting with the laser-irradiated ES is constructed. It is then proved that the ARF acting on the irradiated ES can be controlled by the incident laser beam and that the ARF can be tuned from

*wudajian@njnu.edu.cn

†liuxiaojun@nju.edu.cn

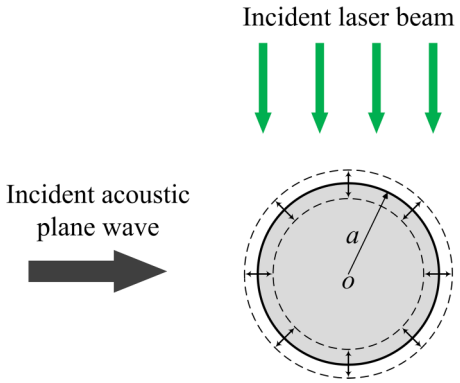

FIG. 1. Schematic of an ES irradiated by both an acoustic plane wave and a laser beam.

a repulsive state to an attractive state. Using the energy-momentum balance theory, we study the absorbed power, the scattered power, and the asymmetry of the scattered field from the irradiated ES, and then use these properties to discuss the change in the ARF. In addition, we investigate the effects of modulation of both the laser intensity and the phase difference between the laser beam and the acoustic plane wave on the ARF that acts on an irradiated polystyrene (PS) sphere. An effective method for realization of a negative ARF acting on the irradiated PS sphere is also presented.

II. LASER MODULATION OF THE ACOUSTIC RADIATION FORCE ACTING ON AN ELASTIC SPHERE

Figure 1 shows a schematic of the combined action of an acoustic plane wave and a laser beam on an ES of radius a. The ES is irradiated by both a sinusoidally modulated laser beam and an acoustic plane wave. The ARF acting on this irradiated ES will be modulated by the incident laser beam (with a wavelength of 532 nm). In this work, we do not consider the optical radiation force acting on the ES because the optical radiation force on the ES is much weaker than the ARF [16].

A. Photoacoustic properties of an elastic sphere in a liquid

The heat diffusion equation for an ES in a liquid can be expressed as

$$\kappa\nabla^2 T(r,t) + H(r,t) = \rho_s c_p \frac{\partial T(r,t)}{\partial t}, \tag{1}$$

where κ, T, ρ_s, and c_p are the thermal conductivity, the temperature rise, the density, and the heat capacity of the ES, respectively. $H = \bar{\alpha} I_0 e^{-i\omega t}$ represents the laser energy that is deposited in the ES per unit volume and per unit time [30,31], where I_0 is the laser intensity, ω is the modulation frequency, and $\bar{\alpha}$ is the optical absorption coefficient. The laser beam is sinusoidally modulated with a frequency ω and irradiates the ES uniformly. If the thermal diffusion length given by $\sqrt{2\kappa_0/\rho_0 C_p \omega}$ (where κ_0 is the thermal conductivity of the fluid) in water during a modulation period is much smaller than the radius of the PS sphere (given by $\sqrt{2\kappa_0/\rho_0 C_p \omega} \ll a$), then the thermal conduction between the sphere and the fluid during the time period in which sound generation occurs can be neglected [32]. For an ES with a radius of 50 μm, the modulation frequency should be higher than 2 MHz to satisfy the thermal confinement condition. In this work, we consider the modulation frequency to be larger than 5 MHz, which meets the thermal confinement condition, and thus thermal conduction can be ignored, i.e., $\kappa = 0$.

The displacement potential Φ^s that results from the thermal expansion can be obtained using the following equation [30].

$$\left(\nabla^2 - \frac{1}{c_l^2}\frac{\partial^2}{\partial t^2}\right)\Phi^s(r,t) = \frac{K\beta}{\rho_s c_l^2} T(r,t). \tag{2}$$

The Φ^s obtained from the above is

$$\Phi^s(r,t) = \frac{i\bar{\alpha}\beta K I_0}{\rho_s^2 c_p \omega^3}[1 + \hat{A}_s j_0(k_s r)]e^{-i\omega t}, \tag{3}$$

where K, β, and c_l are the bulk modulus, the thermal expansion coefficient, and the longitudinal velocity of the ES, respectively. $k_s = \omega/c_l$ is the longitudinal wave number of the ES, while $j_0(k_s r)$ is a zeroth-order spherical Bessel function. The complex amplitude $\hat{A}_s$ can be expressed as

$$\hat{A}_s = \frac{\hat{\rho}(1 - i\hat{c}\hat{q})}{\left(1 - \hat{\rho} + \hat{\rho}\frac{\tilde{c}^2}{\hat{q}^2}\right)\frac{\sin\hat{q}}{\hat{q}} - \left(1 + \hat{\rho}\frac{\tilde{c}^2}{\hat{q}^2}\right)\cos\hat{q} + i\hat{\rho}\hat{c}\left[\left(1 - \frac{\tilde{c}^2}{\hat{q}^2}\right)\sin\hat{q} + \frac{\tilde{c}^2}{\hat{q}}\cos\hat{q}\right]}, \tag{4}$$

where $\hat{q} = \frac{\omega a}{c_l}$, $\tilde{c} = \frac{2c_t}{c_l}$, $\hat{\rho} = \frac{\rho_s}{\rho_0}$, and $\hat{c} = \frac{c_l}{c_0}$. c_t is the transverse velocity of the ES, while ρ_0 and c_0 are the density and the acoustic velocity of the surrounding medium, respectively.

Acoustic radiation force acting on the irradiated elastic sphere

The incident plane acoustic wave can be expanded to a spherical partial wave and boundary conditions can then be applied to resolve the unknown expansion coefficients of the scattered and interior waves of the ES. The velocity potential functions for the incident plane wave and the scattering wave can be expressed as (5) and (6), respectively [21,22]:

$$\varphi_{\text{inc}} = \varphi_0 e^{-i\omega t}\sum_{n=0}^{\infty}(2n+1)i^n j_n(k_0 r)P_n(\cos\theta), \tag{5}$$

$$\varphi_{\text{sca}} = \varphi_0 e^{-i\omega t}\sum_{n=0}^{\infty}(2n+1)i^n A_{n.s} j_n(k_0 r)P_n(\cos\theta), \tag{6}$$

where j_n is the spherical Bessel function, h_n is the spherical Hankel function, P_n is the Legendre polynomial, and $A_{n.s}$ is the scattering coefficient. The longitudinal wave ϕ and the transverse wave ψ in the ES can be expressed as (7) and (8), respectively [33]:

$$\phi = \phi_0 e^{-i\omega t} \sum_{n=0}^{\infty} i^n (2n+1) B_n j_n(k_l r) P_n(\cos\theta), \quad (7)$$

$$\psi = \psi_0 e^{-i\omega t} \sum_{n=0}^{\infty} i^n (2n+1) C_n j_n(k_t r) P_n(\cos\theta), \quad (8)$$

where $k_l = \omega/c_l$ and $k_t = \omega/c_t$ are the longitudinal and transverse wave numbers, respectively, and B_n and C_n are unknown coefficients. The total velocity potential and the acoustic pressure in the surrounding medium are given by $\varphi_{\text{tot}} = \varphi_{\text{inc}} + \varphi_{\text{sca}}$ and $p_{\text{tot}} = p_{\text{inc}} + p_{\text{sca}} = -i\omega\rho_0\varphi_{\text{tot}}$, respectively. The scattered pressure field of a laser-irradiated ES p_{sca} includes two components: the scattering of the ES and the photoacoustic radiation effect [21,22].

The following three boundary conditions at $r = a$ must be satisfied for the irradiated ES [19–23].

(1) Continuities of the normal fluid and solid displacements:

$$u_{fr} = \begin{cases} u_{ar} + u_{lr}, & n = 0 \\ u_{ar}, & n > 0 \end{cases}, \quad (9)$$

where the normal displacement of the fluid $u_{fr} = \frac{1}{\rho_0\omega^2}\frac{\partial p_{\text{tot}}}{\partial r}$, the radial displacement of the ES caused by the plane wave propagation $u_{ar} = \frac{\partial}{\partial r}[\phi + \frac{\partial}{\partial r}(r\psi)] + rk_t^2\psi$, and the radial displacement of the ES due to thermal expansion $u_{lr} = \frac{\partial \Phi^s(r,t)}{\partial r}$.

(2) Continuities of the normal stress and fluid loading (total pressure):

$$-p_{\text{tot}} = \begin{cases} \sigma_{ar} + \sigma_{lr}, & n = 0 \\ \sigma_{ar}, & n > 0 \end{cases}, \quad (10a)$$

$$\sigma_{ar} = -\lambda k_d^2 \phi + 2\mu \left\{ \frac{\partial^2}{\partial r^2}\left[\phi + \frac{\partial}{\partial r}(r\psi)\right] + k_t^2 \frac{\partial}{\partial r}(r\psi) \right\}, \quad (10b)$$

$$\sigma_{lr} = -\omega^2 \rho_s \left[\Phi^s(r,t) + \frac{1}{k_d^2 r}\left(\frac{2c_t}{c_l}\right)^2 \frac{\partial \Phi^s(r,t)}{\partial r} \right], \quad (10c)$$

where σ_{ar} and σ_{lr} are the stresses acting in the radial direction due to plane wave propagation and thermal expansion, respectively, and λ and μ are Lamé coefficients.

(3) Vanishing of the tangential stress component

$$\sigma_{a\theta} = \mu \left(\frac{2\partial}{\partial r}\left\{ \frac{1}{r}\frac{\partial}{\partial \theta}\left[\phi + \frac{\partial}{\partial r}(r\psi)\right]\right\} + k_t^2 \frac{\partial \psi}{\partial \theta} \right) = 0. \quad (11)$$

For simplicity, the laser beam modulation frequency is assumed to be equal to the frequency of the incident acoustic plane wave. The scattering coefficient $A_{n.s}$ of the irradiated ES can be resolved based on the Cramer rule and is expressed as

$$A_{n.s} = \begin{cases} D_{1,n} + D_{2,n} I_0 e^{i\Delta\varphi}, & n = 0 \\ D_{1,n}, & n > 0 \end{cases}, \quad (12a)$$

where $D_{1,n}$ and $D_{2,n} I_0 e^{i\Delta\varphi}$ correspond to the scattering of the ES and the photoacoustic emission, respectively.

$$D_{1,n} = \frac{\begin{vmatrix} B_1 & d_{12} & d_{13} \\ d_{21} & d_{22} & d_{23} \\ B_2 & d_{32} & d_{33} \end{vmatrix}}{\begin{vmatrix} d_{11} & d_{12} & d_{13} \\ d_{21} & d_{22} & d_{23} \\ d_{31} & d_{32} & d_{33} \end{vmatrix}}, \quad D_{2,n} = \frac{\begin{vmatrix} C_1 & d_{12} & d_{13} \\ d_{21} & d_{22} & d_{23} \\ C_2 & d_{32} & d_{33} \end{vmatrix}}{\begin{vmatrix} d_{11} & d_{12} & d_{13} \\ d_{21} & d_{22} & d_{23} \\ d_{31} & d_{32} & d_{33} \end{vmatrix}},$$

$$x_0 = k_0 a, \quad x_l = k_l a, \quad x_t = k_t a,$$

$$d_{11} = -x_0 h_n'(x_0), \quad d_{12} = x_l j_n'(x_l), \quad d_{13} = n(n+1) j_n(x_t),$$

$$d_{21} = 0, \quad d_{22} = 2 j_n(x_l) - 2x_l j_n'(x_l), \quad d_{23} = \left[x_t^2 + 2 - 2n(n+1)\right] j_n(x_t) + 2x_t j_n'(x_t),$$

$$d_{31} = \frac{\rho_0}{\rho_s} x_t^2 h_n(x_0), \quad d_{32} = \left[2n(n+1) - x_t^2\right] j_n(x_l) - 4x_l j'(x_l),$$

$$d_{33} = 2n(n+1)[x_t j'_n(x_t) - j_n(x_t)],$$

$$B_1 = x_0 j_n'(x_0),$$

$$B_2 = -\frac{\rho_0}{\rho_s} x_t^2 j_n(x_0),$$

$$C_1 = \frac{-i\rho_0 \bar{\alpha}\beta K \hat{A}_s (x_l \cos x_l - \sin x_l)}{p_0 \rho_s^2 C_p \omega x_l},$$

$$C_2 = \frac{i\rho_0 x_t^2 \bar{\alpha}\beta K}{p_0 \rho_s^2 C_p \omega}\left[1 + \frac{\hat{A}_s \sin x_l}{x_l} + \frac{1}{x_l^2}\left(\frac{2c_t}{c_l}\right)^2 \left(\cos x_l - \frac{\sin x_l}{x_l}\right)\hat{A}_s\right]. \quad (12b)$$

When the laser beam reaches the PS sphere, the laser phase on the PS sphere is defined as φ_1. The temperature of the PS sphere then rises rapidly, which results in thermal expansion of the sphere. The vibration of the PS sphere is constantly out of phase with the optical modulation [30,31], which means that there is a phase lag donated by $\Delta\delta$ between the photoacoustic signal and the incident laser beam on the PS sphere. However, when the incident acoustic plane wave reaches the SP sphere, the phase of the acoustic wave on the PS sphere is defined as φ_2. If we assume that the acoustic wave phase φ_2 lags by $\Delta\delta$ behind the laser beam phase φ_1, the photoacoustic signal should then be in phase with the incident acoustic plane wave. Here, we define the phase difference between the incident laser beam and the acoustic plane wave as $\Delta\varphi = \varphi_2 - \varphi_1$. In fact, $\Delta\varphi$ determines the phase difference between the photoacoustic signal and the incident plane acoustic wave.

The time-averaged ARF F_x on the ES along the propagation direction can be expressed as $F_x = E_0 S Y_p$, where $E_0 = p_0^2/(2\rho_0 c_0^2)$ represents the energy density of the incident wave, and S is the cross-sectional area of the ES. The dimensional ARF function given by $Y_p = F_x/E_0 S$ is used to evaluate the force acting on the PS sphere and can be expressed as [19–23]

$$Y_p = \frac{-4}{(k_0 a)^2}\sum_{n=0}^{\infty}(n+1)[\alpha_n + \alpha_{n+1} + 2(\alpha_n\alpha_{n+1} + \beta_n\beta_{n+1})], \quad (13)$$

where α_n and β_n are the real and imaginary parts of the scattering coefficient $A_{n.s}$, respectively. Throughout this work, the incident acoustic pressure donated by p_0 is fixed at 500 Pa. We consider a PS sphere (with density $\rho_s = 1050$ kg/m^3, longitudinal sound speed of $c_l = 2350$ m/s, transverse sound speed of $c_t = 1150$ m/s, a bulk modulus of $K = 3.95 \times 10^9$ N/m^2, a thermal expansion coefficient of $\beta = 8 \times 10^{-5}$ 1/K, and an optical absorption coefficient of $\bar{\alpha} = 32.1$ cm^{-1} at 532 nm [34]) in water. The PS sphere radius a is fixed at 50 μm. For the water, the density $\rho_0 = 1000$ kg/m^3 and the compressional velocity $c_0 = 1480$ m/s.

III. NUMERICAL MODEL OF ACOUSTIC RADIATION FORCE ON LASER-IRRADIATED ELASTIC SPHERE

In the following, we introduce the developed numerical model. The finite element method (using COMSOL MULTIPHYSICS 5.2a software) is used to simulate the ARF acting on the ES [35,36]. A three-dimensional (3D) finite element model that includes an ES and the surrounding fluid is established. The surrounding fluid is assumed to be infinite in the model. A perfectly matched layer and the spherical wave radiation boundary condition are used around the object to eliminate wave reflections. Two modules are used in this model: a structural mechanics module and a pressure acoustic module. In the structural mechanics module, a thermal expansion node is added to allow the thermal expansion of the ES to be calculated. In addition, the alternating component of the temperature variation is specified within the thermal expansion node to indicate the temperature rise in the PS sphere, which corresponds to a uniform heat source in the PS sphere. In the pressure acoustic module, an acoustic plane wave with amplitude p_0 propagates along the x direction; this is defined as the background pressure field. At the solid-fluid interface, the boundary condition for the acoustic-structure interaction is used to couple the structural mechanics module and the pressure acoustic module to enable calculation of the photoacoustic emission and the acoustic scattering [29]. The time-averaged ARF F_x that acts on the ES along the propagation direction can be calculated using [37,38]

$$F_x = \int_{s_0}\left[\frac{\rho_0}{4}(|v_y|^2 + |v_z|^2 - |v_x|^2)dA_x - \frac{|p|^2}{4\rho_0 c_0^2}dA_x - \frac{\rho_0}{2}\mathrm{Re}(v_y v_x^*)dA_y - \frac{\rho_0}{2}\mathrm{Re}(v_z v_x^*)dA_z\right], \quad (14)$$

where S_0 is the closed surface of the ES. The dimensional ARF function $Y_p = F_x/E_0 S$ is then used to evaluate the force acting on the PS sphere.

IV. RESULTS AND DISCUSSION

The solid line in Fig. 2(a) shows the ARF function Y_p of a PS sphere as a function of frequency, based on Eq. (13). In this case, the intensity of the incident laser beam $I_0 = 0$. It is observed that the ARFs that act on the PS sphere are always positive, which corresponds with the results of previous reports [39,40]. The apparent peaks are related to the resonances of the PS sphere [41,42]. In Fig. 2(a), the circle scatterers represent simulated ARFs on the PS sphere ($I_0 = 0$) and they match the analytical results well. Figure 2(b) shows the amplitude and phase lag $\Delta\delta$ of the photoacoustic pressure field as a function of optical modulation frequency. Here, $I_0 = 0.1$ mW/μm^2. The photoacoustic pressure amplitude at the PS sphere's surface is calculated using $P_{pa} = \omega^2\rho_s[\Phi^s(a,t) + \frac{1}{k_d^2 a}(\frac{2c_t}{c_l})^2\frac{\partial\Phi^s(a,t)}{\partial a}]$ [30]. Analysis shows that the pressure amplitude and the phase lag are both dependent on the modulation frequency. The maximum pressure occurs at the PS sphere's radial eigenfrequency [30]. Figure 2(c) shows the ARF function Y_p on the laser-irradiated PS sphere as a function of frequency. Here, the laser intensity $I_0 = 0.1$ mW/μm^2, while $\Delta\varphi$ is assumed to be equal to $\Delta\delta$; this means that the photoacoustic signal is in phase with the incident acoustic plane wave. We find that the laser irradiation can affect the ARF acting on the irradiated PS sphere, but the resonance frequencies remain unchanged. The thermoelastic effect induces vibration in the PS sphere, thus meaning that the ARF acting on the irradiated PS sphere can be modulated effectively. In particular, attractive ARFs can be found at some specific frequencies at which the specially required vibrations of the irradiated PS sphere are achieved. In Fig. 2(c), the circle scatterers represent simulated ARFs on the irradiated PS sphere (where $I_0 = 0.1$ mW/μm^2); these results agree well with the analytical results.

The ARF is well known to be the result of momentum transfer from a wave to a particle, and is related to the acoustic field distribution around that particle [15,22,43]. Using the energy-momentum balance theory that was developed by Zhang and Marston [43–45], Eq. (13) can be deduced

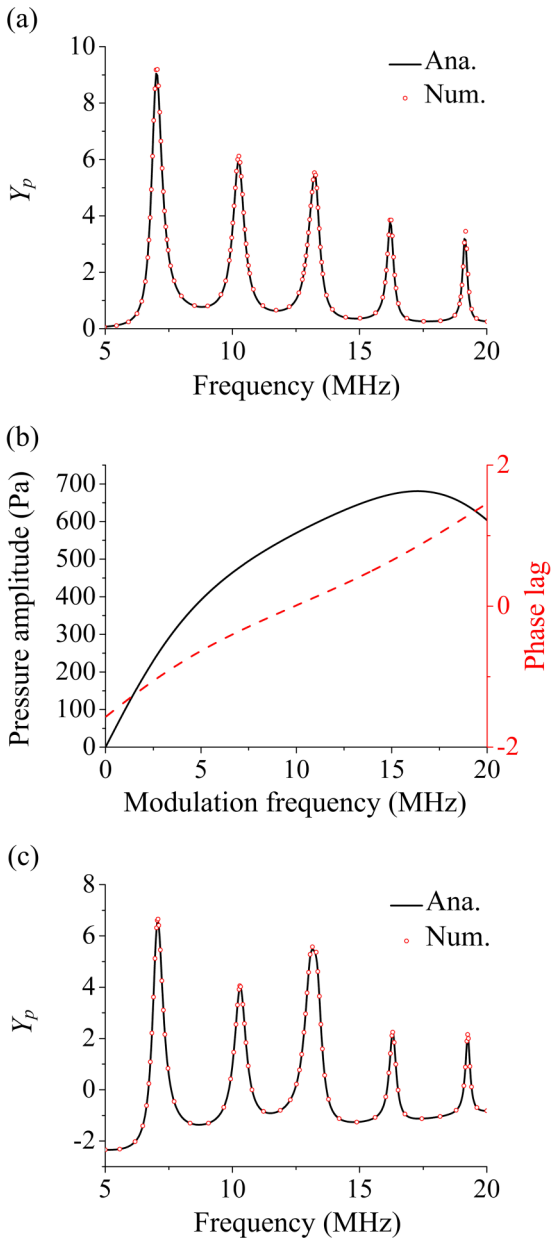

FIG. 2. (a) Analytical and numerical ARF function Y_p curves of the passive PS sphere ($I_0 = 0$) as a function of frequency. (b) Amplitude and phase lag of the photoacoustic pressure of a PS sphere in water as a function of frequency. (c) Analytical and numerical ARF function Y_p curves of the irradiated PS sphere ($I_0 = 0.1\ \mathrm{mW}/\mu\mathrm{m}^2$) as a function of frequency. Here, $\Delta\varphi$ is assumed to be equal to $\Delta\delta$; This means that the photoacoustic signal is in phase with the incident acoustic plane wave.

to be $Y_p = -Q_{\mathrm{sca}}\langle\cos\theta\rangle_s + Q_{\mathrm{ext}}$, where Q_{sca} and Q_{ext} are the scattering and extinction coefficients, respectively. The factor $\langle\cos\theta\rangle_s$ is the asymmetry parameter for the scattering, and provides an axial projection of the scattered momentum. $-Q_{\mathrm{sca}}\langle\cos\theta\rangle_s$ is associated with the asymmetry of the scattered field and is dependent on the momentum that is carried away by the scattering. The second component $Q_{\mathrm{ext}} = Q_{\mathrm{sca}} + Q_{\mathrm{abs}}$ [46], where Q_{abs} is the absorption coefficient. The asymmetry factor $\langle\cos\theta\rangle_s$, the scattering coefficient Q_{sca}, and the absorption coefficient Q_{abs} can be expressed as shown in (15)–(17), respectively, as [43]

$$\langle\cos\theta\rangle_s = \left[8/\left(Q_{\mathrm{sca}}k_0^2a^2\right)\right]\sum_{n=0}^{\infty}(n+1)(\alpha_n\alpha_{n+1} + \beta_n\beta_{n+1}), \tag{15}$$

$$Q_{\mathrm{sca}} = \left[4/\left(k_0^2a^2\right)\right]\sum_{n=0}^{\infty}(2n+1)|A_{n.s}|^2, \tag{16}$$

$$Q_{\mathrm{abs}} = \left[1/\left(k_0^2a^2\right)\right]\sum_{n=0}^{\infty}(2n+1)(1-|1+2A_{n.s}|^2). \tag{17}$$

It always holds that $Q_{\mathrm{sca}} \geqslant 0$ and $Q_{\mathrm{sca}}\langle\cos\theta\rangle \leqslant Q_{\mathrm{sca}}$. Figure 3(a) shows the scattering and absorption coefficients of the PS sphere as functions of frequency. It is observed that the absorption coefficients of the nodissipative PS sphere are always zero and thus the corresponding Y_p values must be positive [45]. Figure 3(b) presents the scattering and absorption coefficients of the laser-irradiated PS sphere as a function of frequency, where $I_0 = 0.1\ \mathrm{mW}/\mu\mathrm{m}^2$. The scattering from the irradiated PS sphere is always positive and is enhanced. Simultaneously, the absorption of the irradiated PS sphere becomes negative, which means that acoustic energy generation is occurring at the irradiated PS sphere, rather than absorption. The maximum absorption occurs at the radial eigenfrequency of the PS sphere, which corresponds to that of the photoacoustic pressure shown in Fig. 2(b). Figures 3(c) and 3(d) show the asymmetric factor $\langle\cos\theta\rangle_s$ for the PS sphere and for the irradiated PS sphere, respectively. When compared with the PS sphere, the asymmetry of the scattered field from the irradiated PS sphere decreases at each frequency because the scattered field is mainly affected by the photoacoustic radiation. If $|Q_{\mathrm{abs}}| > |-Q_{\mathrm{sca}}\langle\cos\theta\rangle_s + Q_{\mathrm{sca}}|$, then the Y_p value becomes negative. Therefore, the ARF acting on the irradiated PS sphere is determined by the competition between the photoacoustic emission and the acoustic scattering. If the photoacoustic effect has a stronger influence than the acoustic scattering of the PS sphere, the ARF will be negative. However, the ARF is positive.

Next, we investigate the effect of the laser intensity on the ARF that is acting on the irradiated PS sphere. Figure 4(a) shows a contour plot of the Y_p curves of the irradiated PS sphere as a function of laser intensity I_0. Here, the phase difference $\Delta\varphi$ between the incident laser beam and the acoustic plane wave is still equal to the phase lag of the photoacoustic signal. The resonance frequencies are also the same as those that were observed in Fig. 2(a). It is found that, with increasing laser intensity, most of the ARFs acting on the irradiated PS sphere could be reduced from positive values to negative values. At certain resonant frequencies, the scattering coefficient becomes very strong and thus higher laser intensities are required to realize these negative ARFs. Figure 4(b) shows a contour plot of the curves for the absorption coefficient Q_{abs} of the irradiated PS sphere as a function of I_0. For the PS sphere (where $I_0 = 0$), the absorption is zero. As the laser intensity increases, increasing amounts of the laser energy are absorbed by the PS sphere and the photoacoustic emission energy is thus increased, resulting in a reduction in

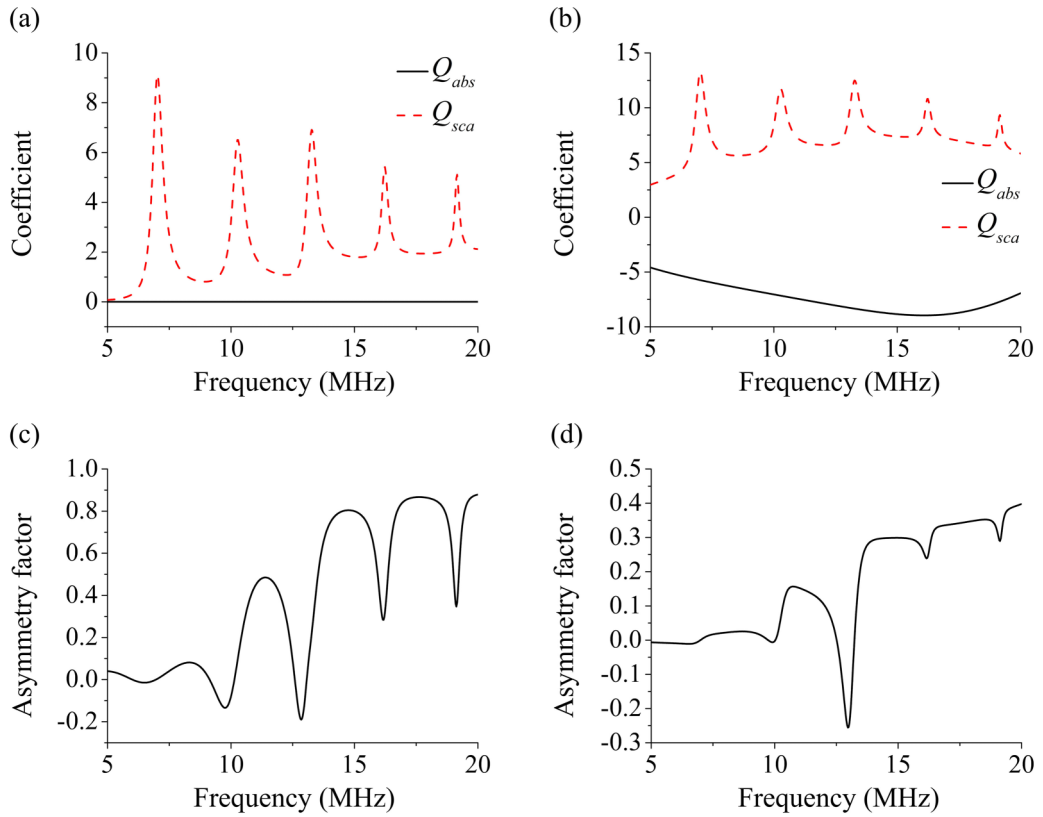

FIG. 3. Scattering and absorption coefficients of the (a) PS sphere ($I_0 = 0$) and (b) the irradiated PS sphere ($I_0 = 0.1\ \mathrm{mW}/\mu\mathrm{m}^2$) as functions of frequency. Variations of asymmetry factor $\langle\cos\theta\rangle_s$ of (c) the passive PS sphere and (d) the irradiated PS sphere with the frequency.

the negative Q_{abs} value. Figure 4(c) shows a contour plot of the curves for the scattering coefficient Q_{sca} of the irradiated PS sphere as a function of I_0. As the laser intensity increases, the scattering of the irradiated PS sphere is enhanced as a result of the increased photoacoustic radiation. When the laser intensity is high enough, the maximal Q_{sca} occurs at the radial eigenfrequency of the PS sphere. Under this condition, the scattering from the irradiated PS sphere is dominated by photoacoustic radiation. Figure 4(d) shows the factor $\langle\cos\theta\rangle_s$ of the scattered field as a function of both I_0 and frequency. It is obvious from the figure that the $\langle\cos\theta\rangle_s$ value at each frequency is modulated by the laser intensity. This means that the scattered field distribution from the irradiated PS sphere must be modified by the photoacoustic radiation. Therefore, the absorption coefficient, the scattering coefficient, and the scattering field distribution of the irradiated PS sphere can all be modified by the laser intensity, thus indicating that the ARF could also be modulated effectively.

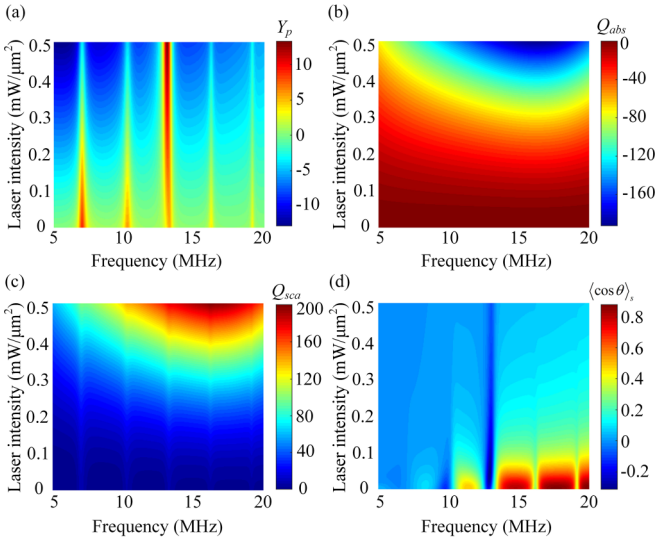

FIG. 4. Contour plots of the (a) Y_p, (b) Q_{abs}, (c) Q_{sca}, and (d) $\langle\cos\theta\rangle_s$ of the irradiated PS sphere as functions of the laser intensity and frequency. Here, $\Delta\varphi$ is assumed to be equal to $\Delta\delta$.

Further discussion of the effects of the phase difference $\Delta\varphi$ between the incident laser beam and the plane acoustic wave on the ARF acting on the irradiated PS sphere is required. Ultimately, $\Delta\varphi$ determines the phase difference between the photoacoustic radiation and the incident plane acoustic wave. Figure 5(a) shows a contour plot of the curves of Y_p for the irradiated PS sphere as a function of $\Delta\varphi$. Here, $\Delta\varphi$ varies from $-\pi$ to π while I_0 remains fixed at $0.1\ \mathrm{mW}/\mu\mathrm{m}^2$. It is found that the ARF acting on the irradiated PS sphere could easily be changed by regulating the phase difference $\Delta\varphi$. Attractive ARFs can be realized at almost all frequencies if the phase difference $\Delta\varphi$ is located within an appropriate range. For example, at a frequency of 13 MHz, the Y_p value of the irradiated PS sphere is a positive value of ~ 6 when $\Delta\varphi = 0$. However, if $\Delta\varphi$ changes from 0 to π, the corresponding Y_p value then becomes a negative value of approximately -0.1. Figures 5(b)–5(d) depict the variations in Q_{sca}, Q_{abs}, and

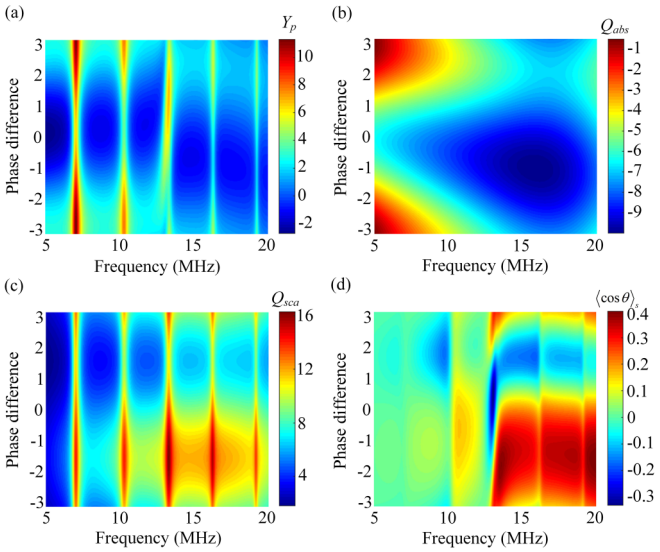

FIG. 5. Contour plots of the (a) Y_p, (b) Q_{abs}, (c) Q_{sca}, and (d) $\langle\cos\theta\rangle_s$ of the irradiated PS sphere as functions of the phase difference $\Delta\varphi$ and frequency. Here, $I_0 = 0.1\ \mathrm{mW}/\mu\mathrm{m}^2$.

$\langle\cos\theta\rangle_s$, respectively, as functions of $\Delta\varphi$ and frequency. It is observed from the figures that Q_{sca}, Q_{abs}, and $\langle\cos\theta\rangle_s$ are all sensitive to changes in $\Delta\varphi$. Therefore, the absorption coefficient, the scattering coefficient, and the scattering field distribution of the irradiated PS sphere could also be modulated using $\Delta\varphi$, thus indicating that the negative ARF could also be modified using $\Delta\varphi$.

Finally, we consider the combined action of the laser intensity I_0 and the phase difference $\Delta\varphi$ on the ARF that acts on the irradiated PS sphere. Figure 6 shows contour plots of the ARF function Y_p of the irradiated PS sphere at frequencies of (a) 10 MHz and (b) 20 MHz as functions of I_0 and $\Delta\varphi$. It is found that both I_0 and $\Delta\varphi$ could modulate the ARF acting on the irradiated PS sphere simultaneously. A negative ARF acting on the irradiated PS sphere could easily be realized by varying I_0 and $\Delta\varphi$. We also note that use of a suitable $\Delta\varphi$ value is most important in enabling a negative ARF to be achieved. As shown in Fig. 6, when the $\Delta\varphi$ value is located in the blue region enclosed by the dashed line, a negative ARF can be realized and the value of the ARF can be modified by varying the laser intensity. If the phase difference is located outside this region, it is then impossible to achieve the negative ARF. Therefore, the most effective method that can be used to control the negative ARF is to maintain a suitable phase difference while simply varying the laser intensity. In addition, it is observed that the region in which the phase difference for the negative ARF occurs is also dependent on the frequency.

V. CONCLUSIONS

We have proposed an alternative method to modulate the ARF acting on the ES using laser irradiation. It is demonstrated that the laser-induced photoacoustic effect on a PS sphere could strongly affect the ARF from the plane acoustic

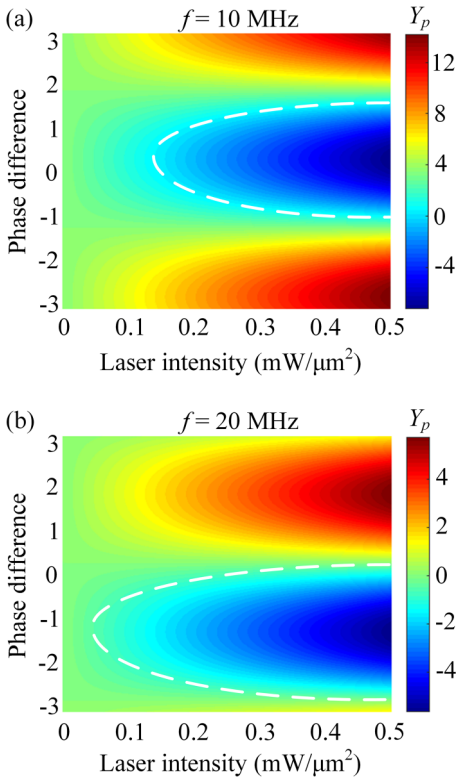

FIG. 6. Contour plots of the ARF function Y_p of the irradiated PS sphere at frequencies of (a) 10 MHz and (b) 20 MHz as functions of the laser intensity I_0 and phase difference $\Delta\varphi$.

wave that acts on the PS sphere and thus negative ARFs can be realized. The tunable nature of the ARF that acts on the irradiated PS sphere is ascribed to competition between the photoacoustic emission and the acoustic scattering. We also investigated the effects of the laser intensity and the phase difference between the incident laser beam and the plane acoustic wave on the ARF that acts on the irradiated PS sphere. It is found that the absorption coefficient, the scattering coefficient, and scattering field distribution of the irradiated PS sphere can all be modulated via the laser intensity and the phase difference. The most effective method to enable control of the negative ARF is to maintain a suitable phase difference while simply varying the laser intensity. The work presented here may open up different avenues for acoustic manipulation of materials.

ACKNOWLEDGMENTS

This work was supported by the National Natural Science Foundation of China (Grants No. 11874222, No. 11674175, and No. 11834008), "333" Project of Jiangsu Province (Grant No. BRA2017451), Major Project of Nature Science Research for Colleges and Universities in Jiangsu Province (Grant No. 15KJA140002), and Postgraduate Scientific Research and Innovation Project of Jiangsu Province (Grant No. KYCX18_1183).

[1] S. F. Chang, T. Si, S. W. Zhang, M. A. Merrick, D. E. Cohn, and R. X. Xu, Ultrasound-mediated destruction of contrast microbubbles used for medical imaging and drug delivery, Ultrason. Sonochem. **28**, 31 (2016).

[2] X. Y. Ding, Z. L. Peng, S. C. S. Lin, M. Geri, S. X. Li, P. Li, Y. C. Chen, M. Dao, S. Suresh, and T. J. Huang, Cell separation using tilted-angle standing surface acoustic waves, P. Natl. Acad. Sci. USA **111**, 12992 (2014).

[3] C. Bouyer, P. Chen, S. Guven, T. T. Demirtas, T. J. F. Nieland, F. Padilla, and U. Demirci, A bio-acoustic levitational (BAL) assembly method for engineering of multilayered, 3D brain-like constructs, using human embryonic stem cell derived neuroprogenitors, Adv. Mater. **28**, 161 (2016).

[4] M. Prisbrey, J. Greenhall, F. G. Vasquez, and B. Raeymaekers, Ultrasound directed self-assembly of three-dimensional user-specified patterns of particles in a fluid medium, J. Appl. Phys. **121**, 014302 (2017).

[5] A. Ziadloo, J. W. Xie, and V. Frenkel, Pulsed focused ultrasound exposures enhance locally administered gene therapy in a murine solid tumor model, J. Acoust. Soc. Am. **133**, 1827 (2013).

[6] M. A. B. Andrade, A. L. Bernassau, and J. C. Adamowski, Acoustic levitation of a large solid sphere, Appl. Phys. Lett. **109**, 044101 (2016).

[7] A. R. Mohapatra, S. Sepehrirahnama, and K. M. Lim, Experimental measurement of interparticle acoustic radiation force in the Rayleigh limit, Phys. Rev. E **97**, 053105 (2018).

[8] F. G. Mitri, Negative axial radiation force on a fluid and elastic spheres illuminated by a high-order Bessel beam of progressive waves, J. Phys. A: Math. Theor. **42**, 245202 (2009).

[9] T. Kido, T. Hasegawa, and N. Okamura, Mechanisms for the attracting acoustic radiation force on a rigid sphere placed freely in a spherical sound field, Acoust. Sci. Technol. **25**, 439 (2004).

[10] R. R. Wu, K. X. Chen, X. Z. Liu, J. H. Liu, Y. W. Mao, and X. F. Gong, Acoustic radiation force on a double-layer microsphere by a Gaussian focused beam, J. Appl. Phys. **116**, 144903 (2014).

[11] M. Azarpeyvand and M. Azarpeyvand, Acoustic radiation force on a rigid cylinder in a focused Gaussian beam, J. Sound. Vib. **332**, 2338 (2013).

[12] J. Lee, S. Y. Teh, A. Lee, H. H. Kim, C. Lee, and K. K. Shung, Single acoustic beam trapping, Appl. Phys. Lett. **95**, 073701 (2009).

[13] J. Lee and K. K. Shung, Radiation forces exerted on arbitrarily located sphere by acoustic tweezer, J. Acoust. Soc. Am. **120**, 1084 (2006).

[14] L. Shen and C. H. Wang, Revised model for the radiation force exerted by standing surface acoustic waves on a rigid cylinder, Phys. Rev. E **97**, 033103 (2018).

[15] F. G. Mitri and Z. E. A. Fellah, The mechanism of the attracting acoustic radiation force on a polymer-coated gold sphere in plane progressive waves, Eur. Phys. J. E **26**, 337 (2008).

[16] D. Baresch, J. L. Thomas, and R. Marchiano, Observation of a Single-Beam Gradient Force Acoustical Trap for Elastic Particles: Acoustical Tweezers, Phys. Rev. Lett. **116**, 024301 (2016).

[17] A. Marzo, S. A. Seah, B. W. Drinkwater, D. R. Sahoo, B. Long, and S. Subramanian, Holographic acoustic elements for manipulation of levitated objects, Nat. Commun. **6**, 8661 (2015).

[18] A. Marzo, M. Caleap, and B. W. Drinkwater, Acoustic Virtual Vortices with Tunable Orbital Angular Momentum for Trapping of Mie Particles, Phys. Rev. Lett. **120**, 044301 (2018).

[19] M. Rajabi and A. Mojahed, Acoustic manipulation: Bessel beams and active carriers, Phys. Rev. E **96**, 043001 (2017).

[20] M. Rajabi and A. Mojahed, Acoustic manipulation of a liquid-filled spherical shell activated with an internal spherical oscillator, Acta Acust. Acust. **103**, 210 (2017).

[21] M. Rajabi and A. Mojahed, Acoustic radiation force control: Pulsating spherical carriers, Ultrasonics **83**, 146 (2017).

[22] M. Rajabi and A. Mojahed, Acoustic manipulation of oscillating spherical bodies: Emergence of axial negative acoustic radiation force, J. Sound. Vib. **383**, 265 (2016).

[23] M. Rajabi and A. Mojahed, Acoustic manipulation of active spherical carriers: Generation of negative radiation force, Ann. Phys. **372**, 182 (2016).

[24] W. Lu, Q. Huang, K. B. Geng, X. X. Wen, M. Zhou, D. Guzatov, P. Brecht, R. Su, A. Oraevsky, and L. V. Wang, Photoacoustic imaging of living mouse brain vasculature using hollow gold nanospheres, Biomaterials **31**, 2617 (2010).

[25] S. Jeon, J. Kim, J. P. Yun, and C. Kim, Non-destructive photoacoustic imaging of metal surface defects, J. Optics **18**, 114001 (2016).

[26] H. Yang, J. S. Kim, S. Ashkenazi, M. O'Donnell, and L. J. Guo, Optical generation of high frequency ultrasound using two-dimensional gold Nanostructure, Appl. Phys. Lett. **89**, 093901 (2006).

[27] A. Prost, F. Poisson, and E. Bossy, Photoacoustic generation by a gold nanosphere: From linear to nonlinear thermoelastics in the long-pulse illumination regime, Phys. Rev. B **92**, 115450 (2015).

[28] N. I. Grigorchuk, Acoustic oscillations of spherical metallic nanoparticles in dielectric media driven by ultrashort laser pulses, Low Temp. Phys. **37**, 329 (2011).

[29] H. Q. Yu, J. Yao, X. W. Wu, D. J. Wu, and X. J. Liu, Tunable photoacoustic properties of gold nanoshells with near-infrared optical responses, J. Appl. Phys. **122**, 134901 (2017).

[30] M. I. Khan and G. J. Diebold, The photoacoustic effect generated by an isotropic solid sphere, Ultrasonics **33**, 265 (1995).

[31] M. I. Khan and G. J. Diebold, The photoacoustic effect generated by laser irradiation of an isotropic solid cylinder, Ultrasonics **34**, 19 (1996).

[32] V. Zharov, T. Malinsky, and V. Alekhnovich, Photoacoustic manipulation of particles and cells, Rev. Sci. Instrum. **74**, 779 (2003).

[33] G. C. Gaunaurd and H. Uberall, RST analysis of monostatic and bistatic acoustic echoes from an elastic sphere, J. Acoust. Soc. Am. **73**, 1 (1983).

[34] M. F. H. Al-Kadhemy and R. I. Khaleel, Estimated theoretical models for optical constants for CuO_2 doped polystyrene films, Adv. Phys. Theor. Appl. **24**, 57 (2013).

[35] T. Wang, M. Ke, C. Qiu, and Z. Liu, Particle trapping and transport achieved via an adjustable acoustic field above a phononic crystal plate, J. Appl. Phys. **119**, 214502 (2016).

[36] P. Hahn, I. Leibacher, T. Baasch, and J. Dual, Numerical simulation of acoustofluidic manipulation by radiation forces and acoustic streaming for complex particles, Lab Chip **15**, 4302 (2015).

[37] C. Y. Qiu, S. J. Xu, M. Z. Ke, and Z. Y. Liu, Acoustically induced strong interaction between two periodically patterned elastic plates, Phys. Rev. B **90**, 094109 (2014).

[38] H. L. He, S. L. Ouyang, Z. J. He, K. Deng, and H. P. Zhao, Broadband acoustic trapping of a particle by a soft plate with a periodic deep grating, J. Appl. Phys. **117**, 164504 (2015).

[39] T. Hasegawa and K. Yosioka, Acoustic-radiation force on a solid elastic sphere, J. Acoust. Soc. Am. **46**, 1139 (1969).

[40] T. Hasegawa, T. Kido, C. W. Min, T. Lizuka, and C. Matsuoka, Frequency dependence of the acoustic radiation pressure on a solid sphere in water, Acoust. Sci. Technol. **22**, 273 (2001).

[41] M. Rajabi and M. Behzad, On the contribution of circumferential resonance modes in acoustic radiation force experienced by cylindrical shells, J. Sound. Vib. **333**, 5746 (2014).

[42] M. Rajabi and M. Behzad, An exploration in acoustic radiation force experienced by cylindrical shells via resonance scattering theory, Ultrasonics **54**, 971 (2014).

[43] L. K. Zhang and P. L. Marston, Geometrical interpretation of negative radiation forces of acoustical Bessel beams on spheres, Phys. Rev. E **84**, 035601 (2011).

[44] L. K. Zhang and P. L. Marston, Axial radiation force exerted by general non-diffracting beams, J. Acoust. Soc. Am. **131**, EL329 (2012).

[45] P. L. Marston and L. K. Zhang, Unphysical consequences of negative absorbed power in linear passive scattering: Implications for radiation force and torque, J. Acoust. Soc. Am. **139**, 3139 (2016).

[46] L. K. Zhang and P. L. Marston, Acoustic radiation force expressed using complex phase shifts and momentum transfer cross sections, J. Acoust. Soc. Am. **140**, EL178 (2016).